Compact Wideband Circularly Polarized Antenna Array for Satellite Applications

Nasimuddin and Xianming Qing
Institute for Infocomm Research (I²R), A*STAR, Singapore
{nasimuddin; qingxm}@i2r.a-star.edu.sg

***Abstract*— A wideband circularly polarized (CP) 2×2 antenna array is proposed for INMARSAT/GNSS applications. The single-feed antenna element consists of an asymmetric-ring-slotted square patch radiator, an asymmetric-slit-slotted square stacked patch, and a coaxial feeding probe. The miniaturized slotted patches with a grounded shorted circular ring are utilized to generate the CP radiation and the stacked configuration to widen the bandwidth. The presented antenna is implemented using an arrangement of RO4003-dielectric substrate and air gap. The measured 10-dB return loss and 3-dB axial ratio (AR) bandwidths of a 2×2 antenna array prototype at the L-band are 16.8% (1.456 GHz–1.724 GHz) and 10.7% (1.51 GHz–1.68 GHz), respectively; the gain is greater than 11.0 dBic across the 3-dB AR bandwidth. The overall antenna volume is 185 mm × 185 mm × 18.0 mm ($0.931\lambda_0 \times 0.931\lambda_0 \times 0.09\lambda_0$, where λ_0 is free space wavelength at 1.51 GHz).**

***Index Terms*— Antenna array, circular polarization, microstrip antenna, stacked microstrip antenna, wideband antenna, GNSS, INMARSAT, metallic-via, slotted-patch.**

I. INTRODUCTION

Circularly polarized (CP) antennas with both broad bandwidth and high gain have gained significant interest nowadays, primarily owing to their growing significance in advanced wireless systems. Their unique attribute of being orientation-insensitive makes CP antennas highly sought after across a diverse range of wireless applications. These encompass critical domains such as global positioning systems, radio frequency identification, satellite communication, radar systems, RF energy harvesting, and beyond.

Designing a compact, single-feed, wideband, high-gain CP antenna is an inherently challenging endeavor. Achieving the simultaneous excitation of orthogonal modes with equal magnitude and a 90° phase difference across a broad frequency range using a single excitation source presents a challenging task. In response to this challenge, numerous innovative techniques have been developed to enhance CP radiation bandwidth. These approaches include the utilization of stacked patches [1], dual-feed structures [2], sequentially rotated feeding networks [3, 4], multi-feed configurations [5], as well as advanced designs involving multilayered and metamaterial structures [6], among others.

Different types of 2×2 CP antenna array structures were reported in the open literature for higher gain [7-11]. A broadband 2×2 array using a multilayered structure [7] achieved a CP (3-dB AR) bandwidth of 20% and an average gain of 10.7 dBic with an overall antenna array size of $1.181\lambda_0 \times 1.181\lambda_0 \times 0.118\lambda_0$ at 11.8 GHz. A cavity-backed CP antenna array (2×2) based on substrate integrated waveguide (SIW) was reported in [8] to show a 3-dB AR bandwidth of 13% with a maximum gain of 11.5 dBic and the antenna array size of $1.767\lambda_0 \times 1.767\lambda_0 \times 0.106\lambda_0$ at 10.6GHz. In [9], a sequentially rotated fed CP antenna array exhibited 13% 3-dB AR bandwidth and gain of 11.5 dBic with an antenna array size of $1.424\lambda_0 \times 1.424\lambda_0 \times 0.0554\lambda_0$ at 4.75 GHz. A 2×2 CP antenna array was developed for Inmarsat services with a gain of 11 dBic and wideband of 9.9% for 5-dB AR, the overall antenna size is $1.093\lambda_0 \times 1.093\lambda_0 \times 0.0.096\lambda_0$ at 1.518 GHz [10].

In this work, a compact wideband CP antenna array with high gain is studied for GNSS/INMARSAT applications. The single-feed antenna element at the L-band exhibits an impedance bandwidth of 230 MHz (1.50GHz–1.73GHz), CP bandwidth of 164MHz (1.517GHz–1.681GHz) and realized gain of ≥ 7.5 dBic across the CP frequency range. The 2×2 CP antenna array achieves an impedance bandwidth of 16.8% (1.456GHz–1.724GHz), CP bandwidth of 10.7% (1.51 GHz–1.68 GHz), and a boresight gain greater than 11.0 dBic with the variation of 0.5 dB across the AR bandwidth. The design/simulation of the antenna/array structures was done with CST Studio Suite [11].

II. ANTENNA ELEMENT DESIGN

Fig. 1 shows the overall antenna element structure. A radiating square patch (L_r = 43.0 mm) is positioned on the top of the substrate (h_1 = 3.048 mm, ε_r =3.55, $\tan\delta$ = 0.0027). A ring-shaped slot (r = 14.2 mm, r_1 = 8.8 mm, and r_2 = 8.05 mm) as illustrated in Fig. 1(b) is embedded into the corner of the square patch at the location of (-*ll*, *ll*), *ll* = 14.2 mm. A ring slot's inner patch is connected to the antenna ground through a metallic via with a diameter of 1.5 mm. A planar stub (length, d_1 = 16.5 mm and width, w_1 = 9.0mm from the square patch's edge and a coaxial feed probe is located at d_o = 35.0 mm along the *x*-axis. Tuning the length and width of the stub is effective in optimizing the impedance matching at the desired frequency band. A slit-slotted parasitic square patch (L_p = 52.2 mm) as exhibited in Fig. 1(c) is placed on the top of the upper-substrate (h_3 = 1.524 mm, ε_r =3.55, and $\tan\delta$ = 0.0027). For CP radiation, the dimensions of the slits and the slot are chosen to be w_s = 1.5 mm, l_s = 16.9 mm, d_p = 11.0 mm, and the circular slot is located at ($-L_p/4$, $L_p/4$). An airgap (h_2 = 16.0 mm) is implemented to further enhance the bandwidth and gain. The overall antenna size (volume) of the antenna element is 90.0 mm × 90.0 mm × 20 mm.

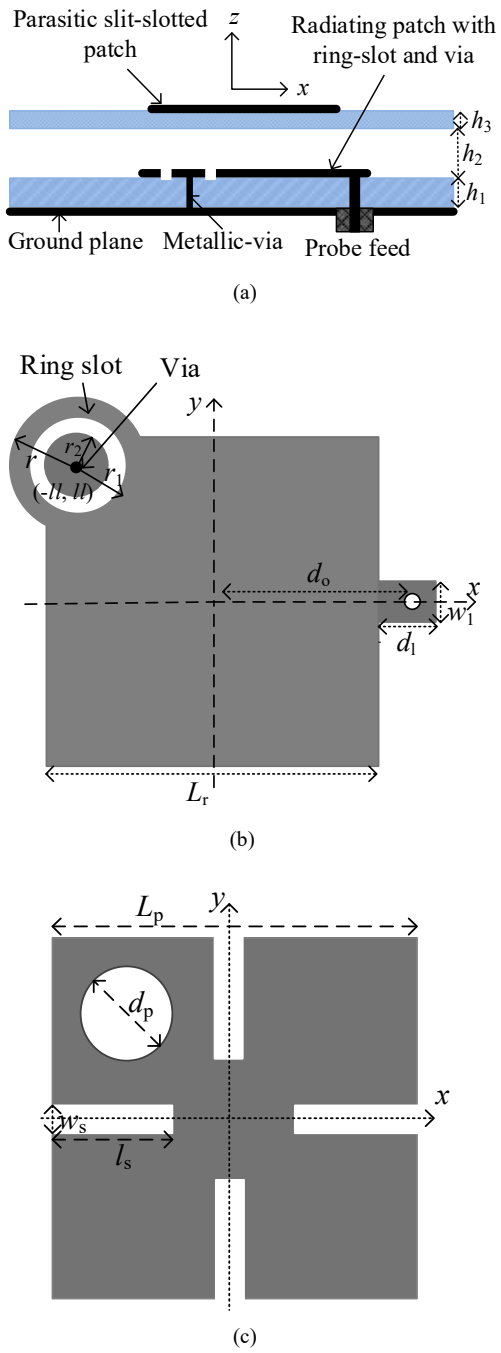

Fig. 1 Proposed stacked slotted-microstrip antenna element: (a) cross-sectional view, (b) ring-slotted square patch with microstrip stub, and (c) slit-slotted square patch.

III. Parametric Study of Antenna Element

A. *The outer radius of the ring-slot, r_1*

The ring-slot with a grounded via is embedded into the radiating square patch to generate CP radiation. The outer radius of the ring slot, r_1, varies from 8.4 mm to 9.2 mm. The AR at the boresight of the element structure with the varying of the ring-slot radius, r_1, is shown in Fig. 2, better AR and desired AR bandwidth are observed when r_1 is 8.8 mm.

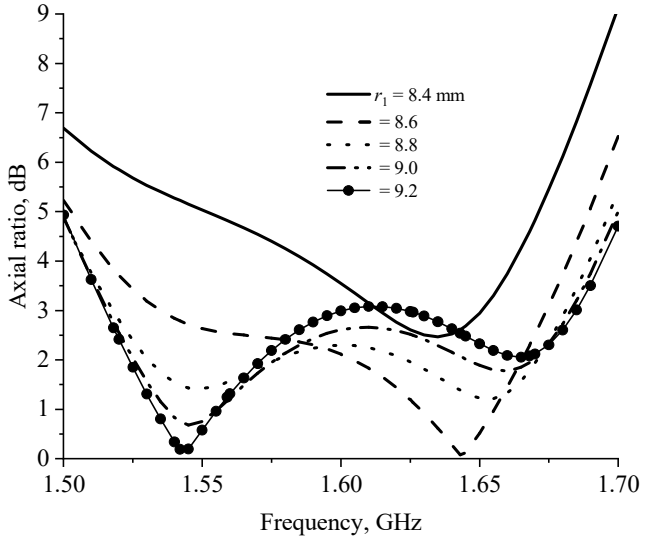

Fig. 2. Simulated AR with a varying outer radius of the ring slot, r_1.

B. *Location (-ll, ll) of the ring-slot*

Fig. 3 shows the AR at the boresight with varying ring-slot locations (-*ll*, *ll*). The grounded-via location is also varied along with the ring slot. For *ll* = 14.2 mm, the antenna confirms respectable CP radiation performance with a larger 3-dB AR bandwidth.

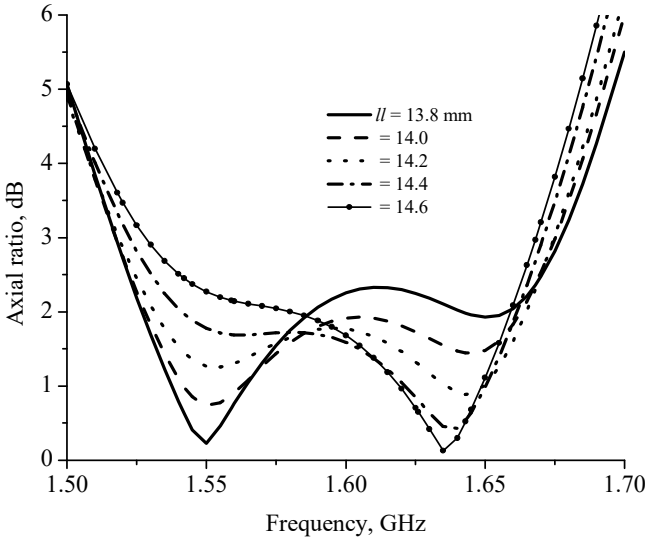

Fig. 3. Simulated AR (boresight) with varying ring-slot location (-*ll*, *ll*).

C. *Ground-plane size, g×g*

The square ground plane of the antenna affects the antenna performance (AR) significantly. The AR at the boreside is plotted in Fig. 4, where the AR shows significant variation with antenna ground plane size and a larger ground plane offers better AR performance.

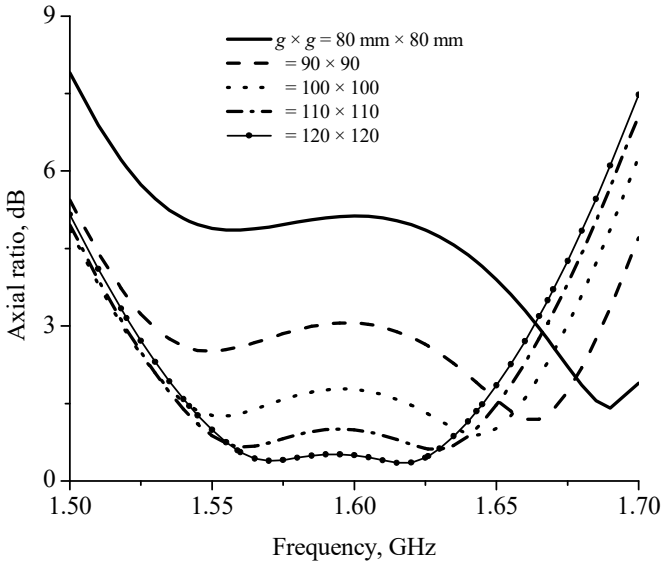

Fig. 4. Simulated AR with varying ground plane size, $g \times g$.

D. ***Feed point location, d_o***

The position of the probe feed spot on the microstrip stub, d_o, is varied from 32 mm to 37 mm. The AR at the boresight shows slight variation with a change in feed location as shown in Fig. 5.

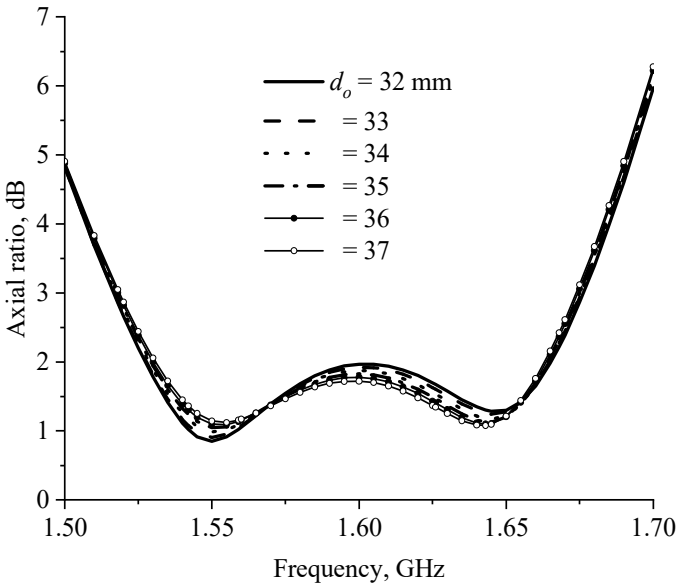

Fig. 5. Simulated AR with feed location, d_o.

IV. 2×2 Antenna Array and Results

Based on the optimized antenna element in Section III, a 2×2 antenna array was formed and prototyped to validate the array structure experimentally. The 2×2 CP antenna array with an inter-element spacing of 110 mm is illustrated in Fig. 6(a), the overall volume is 185 mm × 185mm ×18.0 mm ($0.936\lambda_0 \times 0.936\lambda_0 \times 0.091\lambda_0$ at 1.518 GHz).

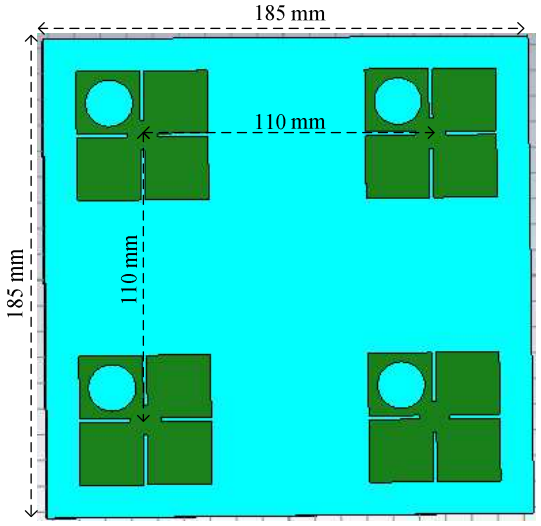

(a)

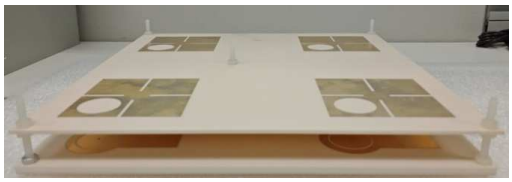

(b)

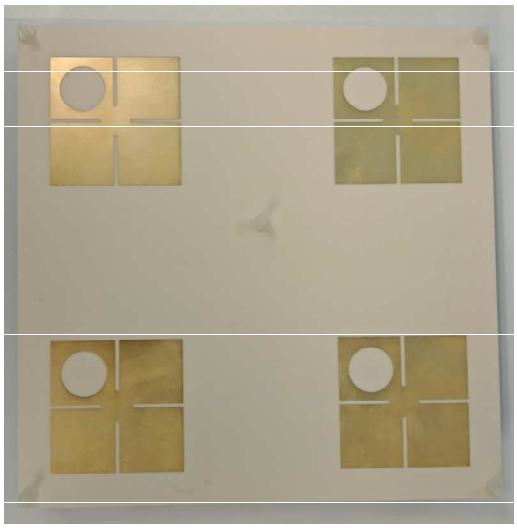

(c)

Fig. 6. 2×2 CP antenna array: (a) simulation layout, (b) side view of the antenna prototype, and (c) top view of the antenna prototype.

To assemble the proposed antenna array structure, five non-metallic holes with a radius of 1.5 mm are created in four corners and around the middle locations of the lower patch radiators substrate and upper patches substrate. Plastic screws with a diameter of 2.5 mm were used to connect the substrates and create the air gap (h_2 = 12.5 mm) between the lower-patch radiator and upper-patch radiator. The photos of the antenna

array prototype (top and side views) are illustrated in Figs. 6(b) and 6(c).

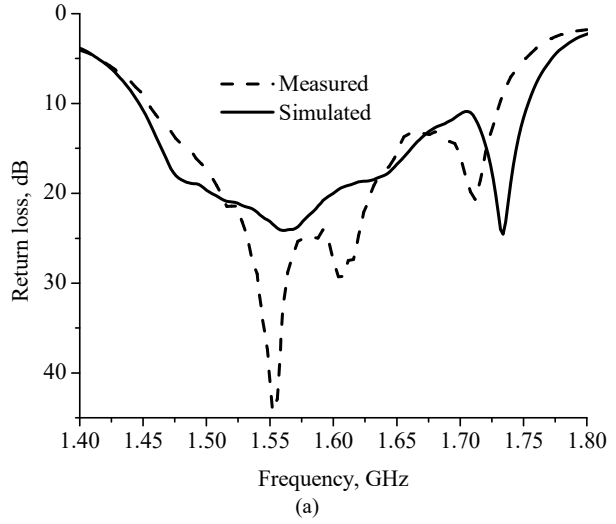

(a)

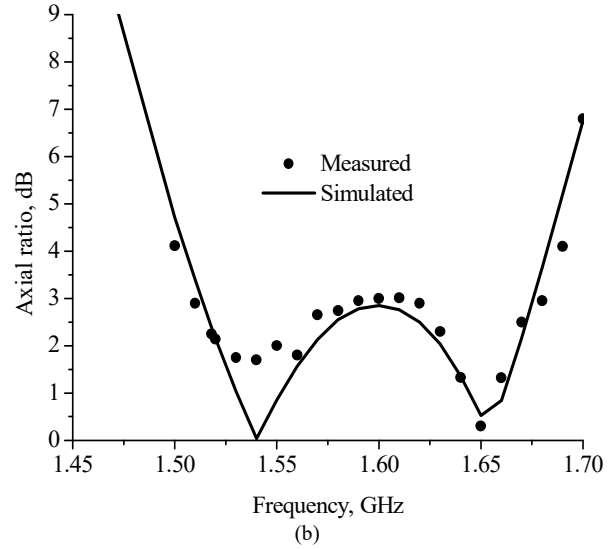

(b)

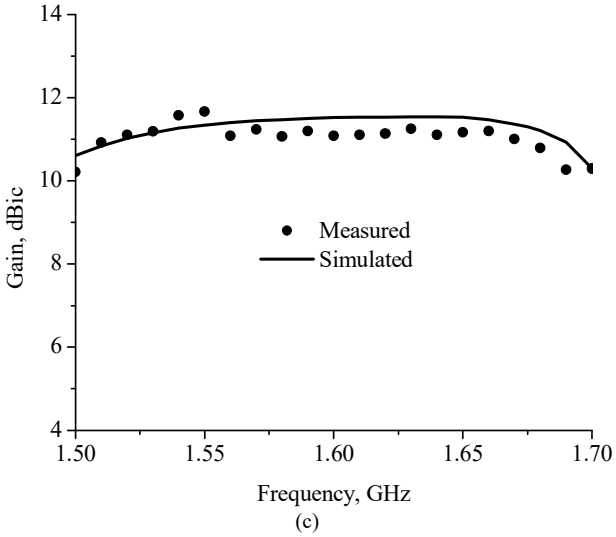

(c)

Fig. 7. Measured and simulated results of the prototype array antenna: (a) return loss, (b) AR (boresight), and (c) realized gain (boresight).

Fig. 7(a) presents a comparison of the simulated and measured return loss for the 2×2 CP antenna array. The measured 10-dB return loss bandwidth impressively spans 16.8%, encompassing frequencies from 1.456 GHz to 1.724 GHz. Notably, there is a good agreement between the simulation and measurement results.

We assessed the antenna's CP performance using a method involving a rotating linear polarized transmitting horn antenna. Fig. 7(b) shows the measured 3-dB AR bandwidth spans 10.7%, covering the frequency range from 1.51 GHz to 1.68 GHz. In Fig. 7(c), we present the measured boresight gain, which consistently exceeds 11.0 dBic across the frequency spectrum, ranging from 1.518 GHz to 1.68 GHz, with a minimal variation of just 0.5 dB. Notably, at 1.55 GHz, the antenna achieves its peak gain of 11.5 dBic.

The measured normalized radiation pattern curves (1.518 GHz, 1.55 GHz, and 1.65 GHz) in *xz*- and *yz*-planes are shown in Fig. 8. The antenna's CP performance can be effectively assessed by analyzing the ripples present in the measured curves. These ripples serve as a visual representation of the AR at specific angles, with smaller ripples indicating superior AR. Furthermore, the 3-dB AR beamwidth extends beyond 90° across the entire 3-dB AR frequency bandwidth. To provide a comprehensive evaluation, we have also included simulated radiation patterns (depicted as dotted lines) in the figures for comparison, and they demonstrate a remarkable alignment with the measured results.

The tested performance of the prototyped 2×2 array structure is assessed in Table I with communicated published 2×2 CP antenna array structures in the literature [7–10] and commercially accessible in the marketplace [10] for INMARSAT applications. With the smallest size, the prototyped antenna array achieves a comparable gain and fulfills the bandwidth requirement for the INMARSAT application (1.51 GHz–1.68 GHz, 10.7%).

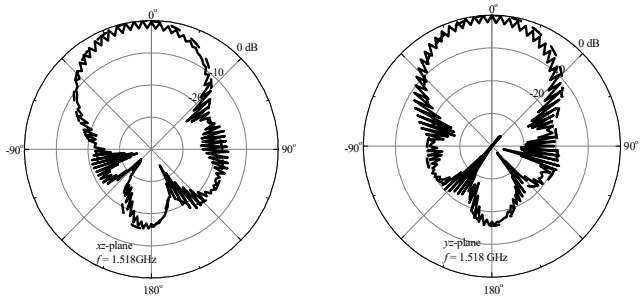

(a)

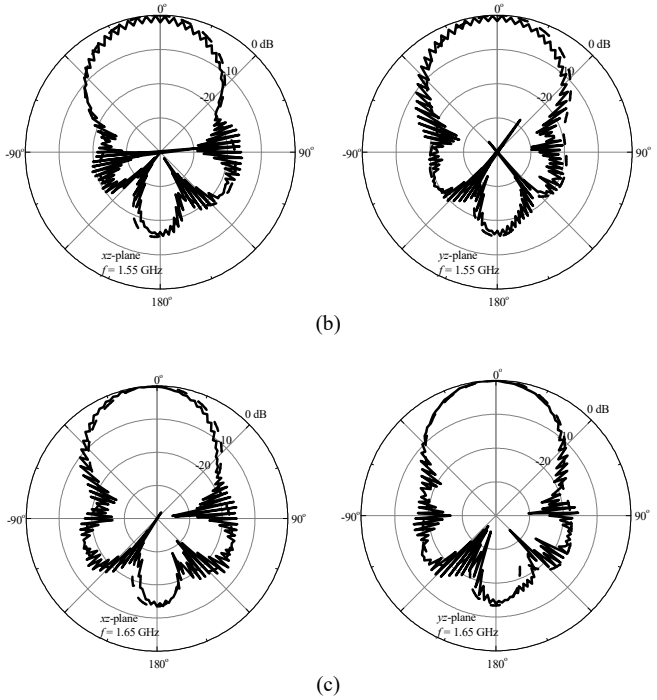

Fig. 8. Normalized measured radiation patterns: (a) 1.518GHz, (b) 1.55GHz, and (c) 1.65GHz.

TABLE I: COMPARISON OF THE WIDEBAND 2×2 CP ANTENNA ARRAYS

Antenna structures	3-dB AR bandwidth (%)	Gain (dBic)	AR	Antenna volume
Proposed antenna	10.7	11.0 (min.)	< 3	$0.936\lambda_0 \times 0.936\lambda_0 \times 0.091\lambda_0$ at 1.518 GHz
[7]	13.0	11.5 (peak)	< 3	$1.767\lambda_0 \times 1.767\lambda_0 \times 0.106\lambda_0$ at 10.6 GHz
[8]	20.0	10.7 (avg.)	< 3	$1.181\lambda_0 \times 1.181\lambda_0 \times 0.118\lambda_0$ at 11.8 GHz
[9]	13.0	11.5 (peak)	< 3	$1.424\lambda_0 \times 1.424\lambda_0 \times 0.0554\lambda_0$ at 4.75 GHz
API Corp.[10]	9.9	11.0 (min.)	< 5	$1.093\lambda_0 \times 1.093\lambda_0 \times 0.096\lambda_0$ at 1.518 GHz

V. CONCLUSION

A miniaturized wideband stacked slotted-patch CP antenna array with high gain has been demonstrated for satellite applications at the L-band. The antenna element was designed/optimized for broadband CP radiation with higher gain. For respectable impedance matching, a planar microstrip stub has been included at the lower slotted square patch radiator with a coaxial probe. The proposed array antenna has confirmed a wideband CP bandwidth with higher gain and is desired for L-band satellite systems.

ACKNOWLEDGMENT

The work was partially supported by the Economic Development Board (EDB), Singapore, under the Office for Space Technology and Industry (OSTIn) Space Technology Development Programme ("STDP") S23-020013-STDP.

REFERENCES

[1] Nasimuddin, K. P. Esselle, and A. K. Verma, "Wideband circularly polarized stacked microstrip antennas", *IEEE Antennas and Wireless Propagation Letters*, vol. 6, pp. 21–24, 2007.

[2] S. D. Targonski and D. M. Pozar, "Design of wideband circularly polarized aperture-coupled microstrip antennas," *IEEE Trans. Antennas and Propagation*, vol. 41, no. 2, pp. 214−220, Feb. 1993.

[3] U. R. Kraft, "An experimental study on 2 × 2 sequential-rotation arrays with circularly polarized microstrip radiators," *IEEE Trans. Antennas and Propagation*, vol. 45, no. 10, pp. 1459−1466, Oct. 1997.

[4] S. Fu, Q. Kong, S. Fang, and Z. Wang, "Broadband circularly polarized microstrip antenna with coplanar parasitic ring slot patch for L-band satellite system application," *IEEE Antennas and Wireless Propagation Letters*, vol. 13, pp. 943−946, 2014.

[5] C. D. Lin, F. Zhang, Y.-C. Jiao, F. Zhang, and X. Xue, "A three-fed microstrip antenna for wideband circular polarization," *IEEE Antennas and Wireless Propagation Letters*, vol. 9, pp. 359–362, 2010.

[6] Nasimuddin, X. Qing, and Z. N. Chen, "Bandwidth enhancement of a single-feed circularly polarized antenna using a metasurface," *IEEE Antennas and Propagation Magazine*, vol. 58, no. 2, pp. 39–46, Apr. 2016.

[7] H. W. Lai, D. Xue, H. Wong, K. K. So, and X. Y. Zhang, "Broadband circularly polarized patch antenna arrays with multiple layers structure, *IEEE Antennas and Wireless Propagation Letters*, vol. 16, pp. 525–528 2016.

[8] D.-F. Guan, B. Fang, Y.-S. Zhang, W. Shao, and J.-H. Shen, "Broadband SIW cavity-backed circularly polarized antenna element and array," *IEEE IWS*, 2015, Jan. 2003.

[9] W. Yang, J. Zhou, Z. Yu, and L. Li, "Bandwidth- and gain-enhanced circularly polarized antenna array using sequential phase feed, *IEEE Antennas and Wireless Propagation Letters*, vol. 13, pp. 1215–1218, 2014.

[10] High gain L-band antenna array, API Technologies Corp., Model RPA11593135CAAF, www.apitech.com.

[11] CST Studio Suite 2023: Version 2023.05-June 2023.